Enhanced photoactivity in nitrogen-doped $KM_{0.33}W_{1.67}O_6$ (M = Al and Cr)

G. Ravi, P. Shrujana, S. Palla, J. R. Reddy, R. Guje, R. Velchuri, M. Vithal

Department of Chemistry, Osmania University, Hyderabad 500 007, India
E-mail: mugavithal@gmail.com

Published in Micro & Nano Letters; Received on 18th October 2013; Revised on 4th December 2013; Accepted on 10th December 2013

The investigation of photocatalysis by efficient visible-light-active photocatalysts has been of interest in both the science and the engineering fields. The nitrogen (N) doped $KAl_{0.33}W_{1.67}O_6$ (KAW) and $KCr_{0.33}W_{1.67}O_6$ (KCW) are prepared by the solid state method. Urea was used as a nitrogen source. These materials were characterised by thermo gravimetric analysis, powder X-ray diffraction, scanning electron microscopy, energy dispersive spectra, X-ray photoelectron spectroscopy (XPS) and UV–visible diffuse reflectance spectroscopy (UV–vis DRS). Both the N-doped materials crystallised in a cubic lattice with space group $Fd\bar{3}m$. The XPS analysis of the N-doped KAW (N-doped KCW) show the characteristic peaks belonging to K 2p, Al 2p (Cr 2p), W 4f, O 1s and N 1s along with C 1s. The bandgap energy was deduced from their UV–vis DRS profiles. The photocatalytic degradation of the methylene blue solution was investigated in the presence of these oxides. Compared with their parent materials, nitrogen doped KAW and KCW samples exhibit ∼230 and ∼130% increase, respectively, in visible light-induced photodegradation of methylene blue.

1. Introduction: Photocatalysis using semiconductors continues to attract the scientific and industrial community because of its potential applications in converting photon (light) energy to chemical energy [1–4]. Titanium dioxide (TiO_2, anatase) with a bandgap of 3.2 eV has been the most accepted and widely used photocatalyst for the mineralisation of various harmful organic compounds and for the successful splitting of water to produce hydrogen and oxygen [1, 5–10]. However, the limitation of TiO_2 is that its photo-excitation occurs only with wavelengths near or shorter than 385 nm. The sunlight, the abundant available energy, has about 4% of UV and ∼40–45% of visible light. Therefore the development of efficient visible-light-active photocatalysts has been an urgent issue from the viewpoint of harvesting solar energy. One way of improving the photocatalytic efficiency is by doping TiO_2 with metal [11–13] and non-metal [14–19] elements to narrow the bandgap energy. The choice of nitrogen (N) as the dopant for the semiconductor oxides has been shown to be promising in photocatalysis. Nitrogen is believed to be the most favourable p-type dopant because of its similar size to oxygen, metastable AX centre formation and small ionisation energy [20]. In general, improved photocatalytic activity for the N-doped oxides is because of the dopant-induced modulation of the electronic structure through the mixing of the N 2p orbitals with the O 2p orbitals within the valence bands (VB), shifting band-to-band threshold excitation energies to longer wavelengths [14]. In the N-doped oxide materials, the holes generated from N 2p by visible light excitation are active species for decomposition of the organic pollutants, although the efficiency of charge separation under visible excitation is lower than that under UV excitation [21, 22].

Defect pyrochlore-type crystalline materials of compositions $AMWO_6$ (A = Rb, Cs; M = Nb, Ta) are found to be promising for water splitting reaction under UV light irradiation because of their wide bandgap energy [23–27]. Lu *et al.* have reported that N-doping in $CsTaWO_6$ has reduced the bandgap from 3.8 to 2.3 eV and exhibited a nearly 100% increase in the hydrogen production efficiency under solar light [28]. Methods of preparation such as sol–gel, heating the oxide in the presence of N-source and ion implantation were developed to prepare nitrogen doped (N-doped) TiO_2 [29]. Sintering the metal oxide with urea at 200–400 °C for ∼2 h is found to be a conventional method of obtaining N-doped metal oxide. This method has been widely used for N-doping of solid acids or metal oxides, such as $H_2Ti_4O_9$, $NaNbO_3$, $H_2Ta_2O_6$ and $KSbWO_6$ and $K_2La_2Ti_3O_{10}$ [30–35]. We have earlier reported the photoactivity studies of cation doped $KM_{0.33}W_{1.67}O_6$ (M = Al and Cr) [36, 37]. In the present Letter, the preparation, characterisation and photocatalytic activity of N-doped $KM_{0.33}W_{1.67}O_6$ (M = Al and Cr) are presented.

2. Experimental: $KAl_{0.33}W_{1.67}O$ (KAW) and $KCr_{0.33}W_{1.67}O_6$ (KCW) were prepared by the sol–gel method [36, 37]. The N-doped KAW ($KAl_{0.33}W_{1.67}O_{6-x}N_y$) and KCW ($KCr_{0.33}W_{1.67}O_{6-x'}N_{y'}$) were obtained by heating a mixture of KAW (KCW) and urea at 400°C for 2 h in a muffle furnace in air. The weight ratio of KAW (KCW) to urea was 1:2. The resultant powder was washed several times with deionised water to remove excess unreacted urea. The colour of the N-doped KAW (KCW) was found to be light yellow (green) and designated as KAWN (KCWN).

Thermogravimetric analysis (TGA) was performed using a Shimadzu differential thermal analyser (DTG-60H) with a heating rate of 15°C min^{-1}. The powder X-ray diffractograms were recorded for phase confirmation on the Shimadzu XRD 7000 powder X-ray diffractometer by using Cu Kα radiation of wavelength 1.5418 Å. The diffractograms were recorded at room temperature in the 2θ range 10–80°. The step size and the scan step time were 0.02° and 0.15 s, respectively. The X-ray photoelectron spectroscopic (XPS) measurements were performed on a KRATOS AXIS165 X-ray photoelectron spectrometer by using an excitation energy of 1253.6 eV (Mg Kα) and a pass energy of 80 eV. SEM images and EDS profiles were recorded on the HITACHI SU-1500 variable pressure scanning electron microscope (VP-SEM). A JASCO V-650 UV–Vis spectrophotometer was used for the UV–vis diffuse reflectance spectra (DRS) measurements in the range of 200–900 nm. $BaSO_4$ was used as the reflectance standard.

The photocatalytic activity of both the KAWN and the KCWN was evaluated by the photodegradation of methylene blue (MB) using a HEBER visible annular type photoreactor (Model: HVAR1234). In a typical process, 50 ml of aqueous MB solution of initial concentration, $C_0 = 1 \times 10^{-4}$ mol/l and 50 mg of the catalyst are taken in a cylindrical quartz tube. The suspension was stirred in the dark for 120 min to establish an adsorption–desorption equilibrium. Then, the solution was exposed to a 300 W tungsten lamp (having the wavelength in the range of 380–840 nm) with continuous air purging. At regular time intervals of 30 min, about 3–5 ml of the solution was collected and filtered through a

Millipore filter to remove the catalyst particles. The change in the concentration of MB was obtained by recording the absorbance on the JASCO V-650 UV–vis spectrophotometer, at 664 nm.

3. Results and discussion: Thermogravimetric (TG) profiles of the KAWN and the KCWN are shown in Fig. 1. These profiles are characterised by two significant weight change regions. In the temperature region 30–450°C, the weight losses are 2.9 and 2.25% for the KAWN and the KCWN, respectively. This weight loss may be attributed to the adsorbed and lattice water as they were extracted from water. In the 450–900°C region, both the samples registered weight gains of 0.20 and 0.28% for the KAWN and the KCWN, respectively. It is well known that the N-doped oxides gain weight on heating to above 500°C because of the release of gaseous nitrogen and become pure oxides [35]. Based on the TG profiles, the molecular formulae of the KAWN and the KCWN can be written as $KAl_{0.33}W_{1.67}O_{5.91}N_{0.06}$ $0.72H_2O$ (wt% of N is 0.18) and $KCr_{0.33}W_{1.67}O_{5.865}N_{0.09}$ $0.57H_2O$ (wt% of N is 0.27), respectively.

The room temperature powder XRD patterns of the parent and the N-doped materials are recorded for phase confirmation. The powder patterns of the KAW and the KAWN are identical (Fig. 2*a*) [36]. Similarly, the powder patterns of the KCW and the KCWN are also alike (Fig. 2*b*) [37]. Nevertheless, a close examination of the d-spacing shows a systematic shift towards a lower 2θ value indicating the substitution of nitrogen into the defect pyrochlore lattice. Nitrogen is known to substitute oxygen in the BO_6 octahedra of the defect pyrochlore lattice [35]. As the ionic radius of N^{3-} (0.171 nm) is higher than that of O^{2-} (0.140 nm) the unit cell parameters should increase resulting in a decrease in the 2θ values. The unit cell parameters of the KAWN and the KCWN are refined by least squares fitting of the powder data by using POWD software. Both the samples crystallised in the cubic lattice with the space group $Fd\bar{3}m$. The obtained unit cell parameters are $a = 10.242$ Å for KAWN and $a = 10.334$ Å for KCWN, respectively. The slight increase in the unit cell parameter of both the oxides compared with their parent compounds is because of partial substitution of N into the $[Al(Cr)/W]O_6$ octahedra of the KAW(KCW) lattice and also incorporation of water into the lattice. The change in the colour of the N-doped oxides compared with their parent oxides also supports the substitution of N into the oxygen sites in the lattice.

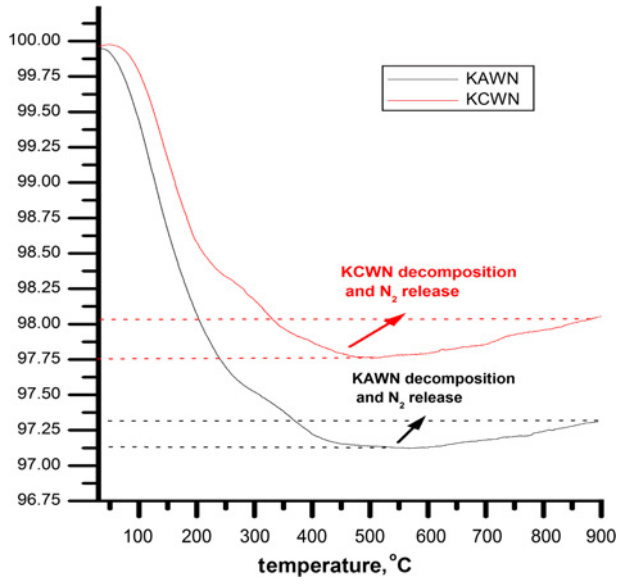

Figure 1 *TGA profiles of the KAWN and the KCWN*

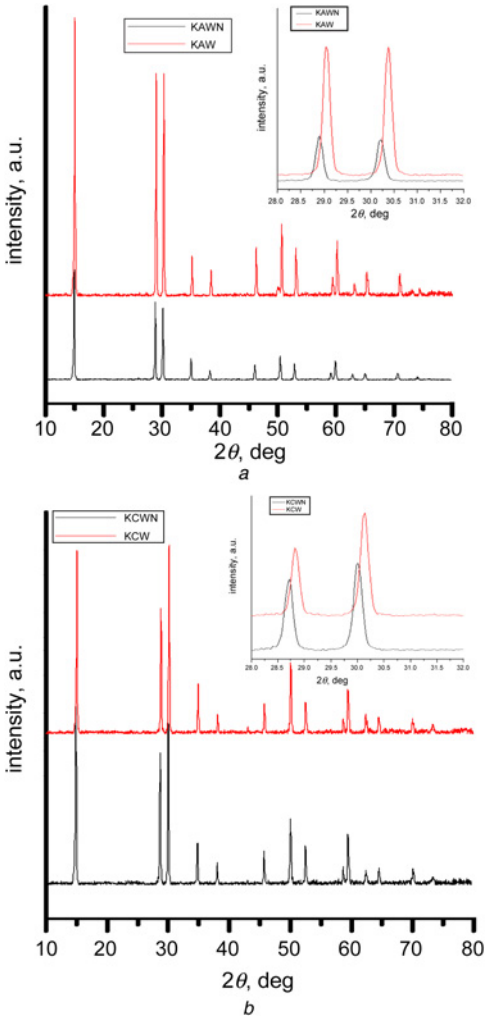

Figure 2 *Powder XRD patterns of the KAWN and the KAW and the KCWN and the KCW.*
a Of the KAWN and the KAW
b Of the KCWN and the KCW

The morphologies of the KAWN and the KCWN were studied by a scanning electron microscope (SEM) (Fig. 3). The SEM images of both the KAWN and the KCWN show irregular size microcrystallites with considerable agglomeration. An estimation of the nitrogen contents in KAWN and KCWN was also obtained from the EDS measurements (Fig. 3). From the area ratio of the elements, the nitrogen contents (in wt%) were found to be 0.21 and 0.32 for KAWN and KCWN, respectively, (Table 1). This result is comparable with the nitrogen weight percentage obtained from the TGA results. Further confirmation of nitrogen doping in the defect pyrochlore lattice was obtained from the XPS measurements (Figs. 4*a* and *b*), in both the spectra exhibit characteristic peaks because of K, Al, Cr, W, N and O along with the C 1s peak. The surface high resolution XPS of the KAWN is characterised by peaks belonging to K 2p, Al 2p, W 4f, O 1s, N 1s and C 1s (Fig. 4*a*). Similarly, the XPS profile of the KCWN was characterised by K 2p, Cr 2p, W 4f, O 1s, N 1s and C 1s peaks (Fig. 4*b*). The C 1s peak appears because of the contamination of the hydrocarbons from air. The presence of the N 1s peak in the XPS of both spectra confirms the N-doping into their lattice. The binding energy of the N 1s is found to be in the range 396–408 eV depending on the environment of the doped site [38]. In the present investigation, the N 1s peak is observed at 399.7 eV for the KAWN (Fig. 4*a*, inset) and 400.8 eV for the KCWN (Fig. 4*b*, inset). These peaks can be assigned to the O–W–N (O-Al(Cr)–N) linkages of the KAWN (KCWN) defect pyrochlore lattice [35].

doi: 10.1049/mnl.2013.0595

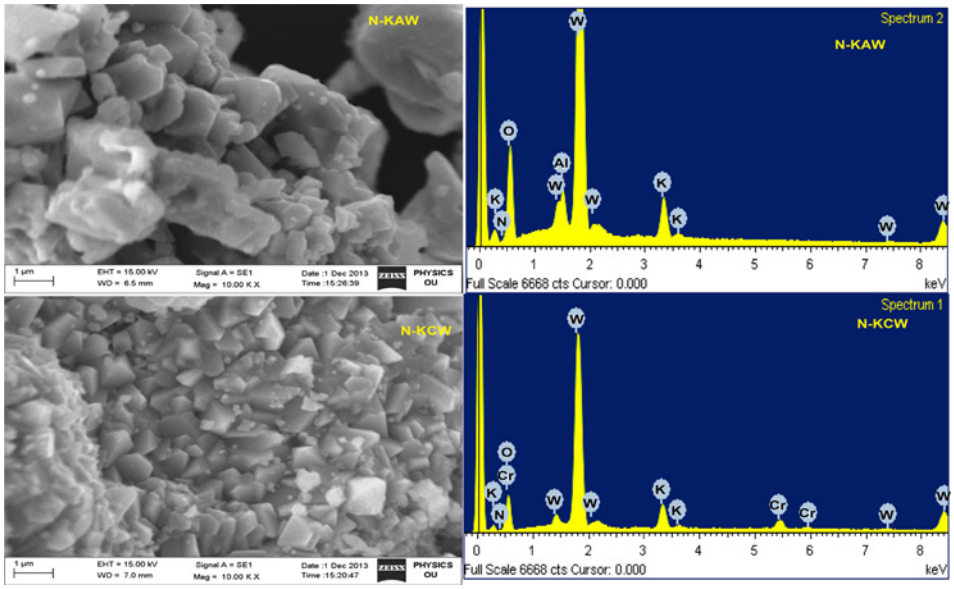

Figure 3 *Scanning electron microscope images and EDS profiles of the KAWN and the KCWN*

Table 1 Energy dispersive spectra data of the KAWN and the KCWN

Element	Weight, %
KAWN	
N K	0.21
O K	20.98
Al K	1.97
K K	8.68
W L	68.16
KCWN	
N K	0.32
O K	20.51
Cr K	3.74
K K	8.53
W L	68.90

The bandgap energies (E_g) of the KAWN and the KCWN were obtained from the Kubelka-Munk plot ($(Khv)^{1/2}$ against hv) (Figs. 5*a* and *b*, respectively). The obtained bandgap energies for the KAWN and the KCWN are 2.52 and 1.87 eV, respectively, which are considerably lower compared with their parent KAW (2.82 eV) and KCW (2.03 eV) defect pyrochlores. The N-induced states (N 2p) localise at a slightly higher energy level than the native oxygen states (O 2p) so that the bandgap of the system is reduced and improved visible light absorption can be expected [39]. The change in the colour of the N-doped samples also confirms a decrease in the E_g value (Fig. 5, insets).

The photocatalytic activities of the KAWN and the KCWN were evaluated by the degradation of the methylene blue (MB) aqueous solution under visible light irradiation. Before the irradiation, both solutions were kept in a dark chamber for the adsorption–desorption equilibrium for 2 h. As shown in Fig. 6*a*, the equilibrium was attained in 1 h. The total adsorbed amount was found to be 4 and

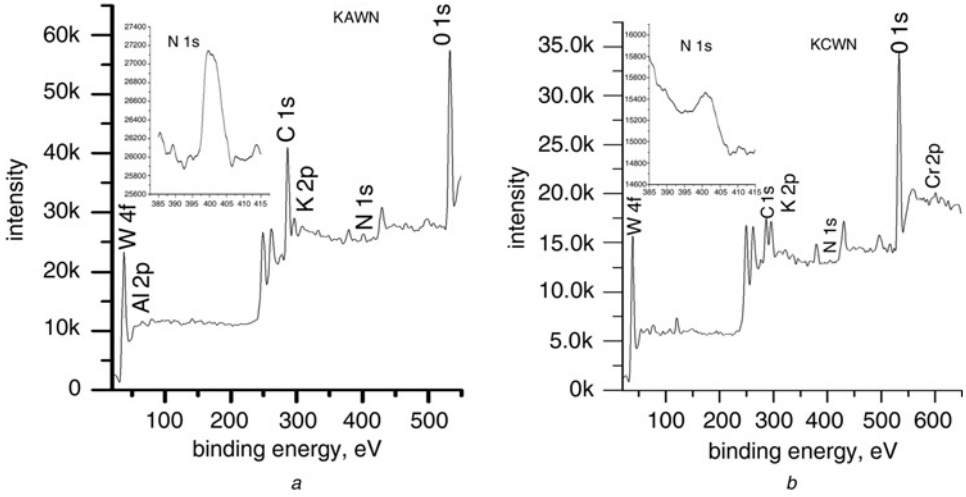

Figure 4 *XPS profiles*
a KAWN (inset, N 1s is the peak of KAWN)
b KCWN (inset, N 1s is the peak of KCWN)

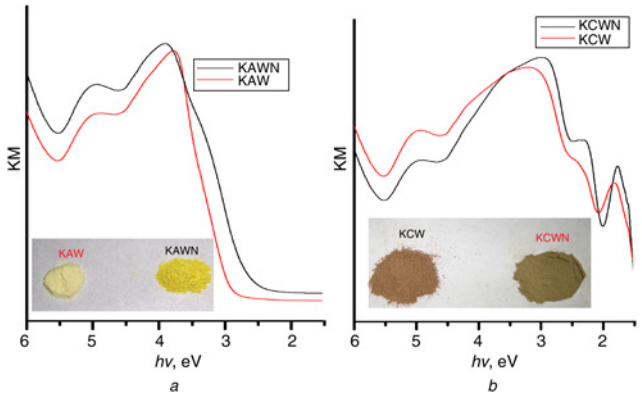

Figure 5 *Kubelka-Munk plots*
a For KAWN and KAW
b For KCWN and KCW
Insets show the colour of the samples

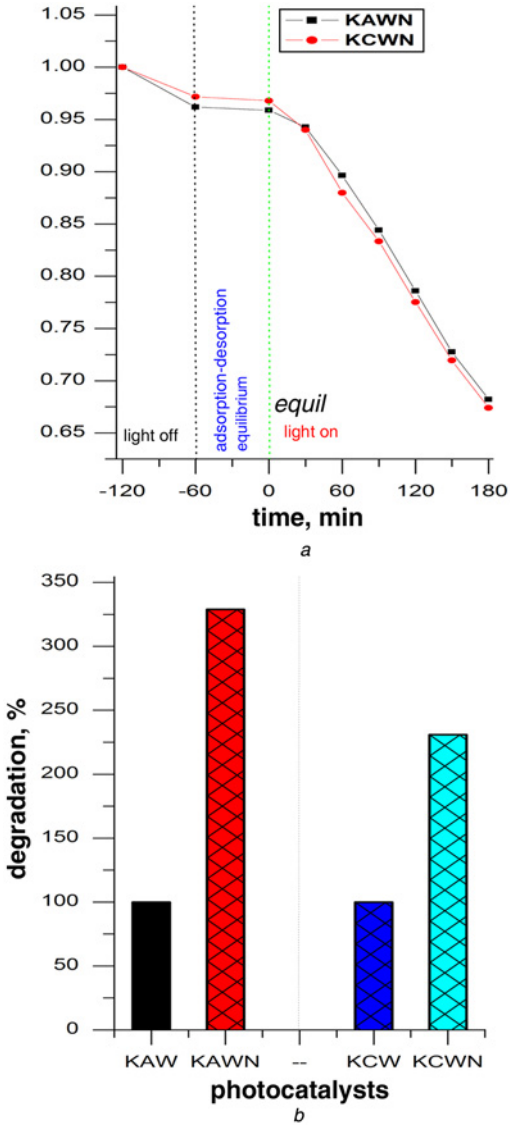

Figure 6 *Photodegradation of the MB in the presence of the KAWN and the KCWN and comparison of the photodegradation of the MB of the N-doped and undoped defect pyrochlores*
a Photodegradation
b Comparison of photodegradation

3% for the KAWN and the KCWN, respectively. Both solutions were irradiated with visible light and the degradation process was monitored by measuring the optical density (at 664 nm) and the UV–vis spectra at regular 30 min intervals. Both the catalysts have shown almost the same activity and degraded about 30% of MB in 3 h. A blank experiment without a catalyst was also performed. Only the MB solution was irradiated with visible light for 3 h. The change in the concentration of MB was found to be negligible (it should be noted that the initial concentration of the MB was 1×10^{-4} mol/l, which is ten times higher compared with our earlier report [36]).

A comparison of the photoactivities of the KAWN and the KCWN with their parent materials ($KAl_{0.33}W_{1.67}O_6$ and $KCr_{0.33}W_{1.67}O_6$) is worth mentioning. It is observed that the photoactivities of the KAWN and the KCWN against the MB were, respectively, 3.3 and 2.3 times higher than the photoactivity of the KAW and the KCW (Fig. 6*b*). The improved photocatalytic activity for both the N-doped oxides may be attributed to (a) a decrease in the bandgap energy of the N-doped defect pyrochlores leading to an increase in the number of the absorbed photons and (b) defects created in the lattice because of the incorporation of nitrogen leading to a decrease in the electron–hole recombination rate. We have also compared the photoactivities of the KAWN and the KCWN with Degussa P25. Both the N-doped materials have shown higher photoactivity compared with that of the Degussa P25. Regarding the MB degradation after 180 min of visible light irradiation in the presence of the Degussa P25, the KAWN and the KCWN follow the order: Degussa P25 < KCWN≃KAWN.

4. Conclusion: Nitrogen doped KAW and KCW were prepared by a facile solid state reaction method using urea as a nitrogen source. The powder XRD patterns confirm their pyrochlore-type structure. Both the samples were crystallised in a cubic lattice. Based on the TGA and the EDS profiles, the nitrogen content was found to be 0.18–0.21 and 0.27–0.32 wt% in the KAW and the KCW, respectively. The incorporation of nitrogen into the defect pyrochlore lattice as O–W–N (O–Al(Cr)–N) is confirmed from (a) the shift in the d-lines of the powder patterns, (b) the presence of N 1s peak in their photo-electron spectra, (c) the change in the colour of the samples and (d) the shift in the absorption edge in the UV–vis DRS profiles. The bandgap energy of the N-doped defect pyrochlores is reduced by about 0.15–0.3 eV. The nitrogen doped KAW (KCW) has shown higher photoactivity against MB degradation in comparison to Degussa P25 under visible light irradiation.

5. Acknowledgments: The authors gratefully acknowledge the UGC (UPE) and the DST (PURSE and FIST), New Delhi, for financial assistance. G. Ravi, thanks the UGC and the RFSMS (Research Fellowship in Science for Meritorious Students), New Delhi, for providing financial support.

6 References

[1] Fox M.A., Dulay M.T.: 'Heterogeneous photocatalysis', *Chem. Rev.*, 1993, **93**, pp. 341–357
[2] Legrini O., Oliveros E., Braun A.M.: 'Photochemical processes for water treatment', *Chem. Rev.*, 1993, **93**, pp. 671–698
[3] Fujishima A., Honda K.: 'Electrochemical photolysis of water at a semiconductor electrode', *Nature*, 1972, **238**, pp. 37–38
[4] Ravelli D., Dondi D., Fagnoni M., Albini A.: 'Photocatalysis. A multi-faceted concept for green chemistry', *Chem. Soc. Rev.*, 2009, **38**, pp. 1999–2011
[5] Pruden A.L., Ollis D.F.: 'Photoassisted heterogeneous catalysis: the degradation of trichloroethylene in water', *J. Catal.*, 1983, **82**, pp. 404–417
[6] Hsiao C.Y., Lee C.L., Ollis D.F.: 'Heterogeneous photocatalysis: degradation of dilute solutions of dichloromethane (CH_2Cl_2), chloroform ($CHCl_3$), and carbon tetrachloride (CCl_4) with illuminated TiO_2 photocatalys', *J. Catal.*, 1983, **82**, pp. 418–423

doi: 10.1049/mnl.2013.0595

[7] Hoffman M.R., Martin S.T., Choi W., Bahnemann D.W.: 'Environmental applications of semiconductor photocatalysis', *Chem. Rev.*, 1995, **95**, pp. 69–96

[8] Linsebigler A.L., Lu G., Yates Jr. J.T.: 'Photocatalysis on TiO_2 surfaces: principles, mechanisms, and selected results', *Chem. Rev.*, 1995, **95**, pp. 735–758

[9] Mills A., Hunte S.L.: 'An overview of semiconductor photocatalysis', *J. Photochem. Photobiol. A*, 1997, **108**, pp. 1–35

[10] Carp O., Huisman C.L., Reller A.: 'Photoinduced reactivity of titanium dioxide', *Prog. Solid State Chem.*, 2004, **32**, pp. 33–177

[11] Choi W., Termin A., Hoffmann M.R.: 'The role of metal ion dopants in quantum-sized TiO_2: correlation between photoreactivity and charge carrier recombination dynamics', *J. Phys. Chem.*, 1994, **98**, pp. 13669–13679

[12] Subramanian V., Wolf E.E., Kamat P.V.: 'Influence of metal/metal ion concentration on the photocatalytic activity of TiO_2-Au composite nanoparticle', *Langmuir*, 2003, **19**, pp. 469–474

[13] Zhu J., Deng Z., Chen F., *ET AL.*: 'Hydrothermal doping method for preparation of Cr^{3+}-TiO_2 photocatalysts with concentration gradient distribution of Cr^{3+}', *Appl. Catal. B*, 2006, **62**, pp. 329–335

[14] Asahi R., Morikawa T., Ohwaki T., Aoki K., Taga Y.: 'Visible-light photocatalysis in nitrogen-doped titanium oxides', *Science*, 2001, **293**, pp. 269–271

[15] Morikawa T., Asahi R., Ohwaki T., Aoki A., Taga Y.: 'Band-gap narrowing of titanium dioxide by nitrogen doping', *Jpn. J. Appl. Phys.*, 2001, **40**, pp. L561–L563

[16] Umebayashi T., Yamaki T., Itoh H., Asai K.: 'Band gap narrowing of titanium dioxide by sulfur doping', *Appl. Phys. Lett.*, 2002, **81**, pp. 454–456

[17] Moon S., Mametsuka H., Tabata S., Suzuki E.: 'Photocatalytic production of hydrogen from water using TiO_2 and B/TiO_2', *Catal. Today*, 2000, **58**, pp. 125–132

[18] Sakthivel S., Kisch H.: 'Photocatalytic and photoelectrochemical properties of nitrogen-doped titanium dioxide', *Chem. Phys. Chem.*, 2003, **4**, pp. 487–490

[19] Sakthivel S., Janczarek M., Kisch H.: 'Visible light activity and photoelectrochemical properties of nitrogen-doped TiO_2', *J. Phys. Chem. B*, 2004, **108**, pp. 19384–19387

[20] Park C.H., Zhang S.B., Wei S.H.: 'Origin of p-type doping difficulty in ZnO: the impurity perspective', *Phys. Rev. B*, 2002, **66**, (1–3), p. 73202

[21] Katoh R., Furube A., Yamanaka K., Morikawa T.: 'Charge separation and trapping in N-doped TiO_2 photocatalysts: a time-resolved microwave conductivity study', *J Phys. Chem. Lett.*, 2010, **1**, pp. 3261–3265

[22] Tang J., Cowan A., Durrant J., Klug D.: 'Mechanism of O_2 production from water splitting: nature of charge carriers in nitrogen doped nanocrystalline TiO_2 films and factors limiting O_2 production', *J Phys. Chem. C*, 2011, **115**, pp. 3143–3150

[23] Ikeda S., Itani T., Nango K., Matsomara V.: 'Overall water splitting on tungsten-based photocatalysts with defect pyrochlore structure', *Catal. Lett.*, 2004, **98**, pp. 229–233

[24] Mitchell I.V.: 'Pillared layered structures: current trends and applications' (Elsevier Applied Science, London, 1990)

[25] Osterloh F.E.: 'Inorganic materials as catalysts for photochemical splitting of water', *Chem. Mater.*, 2008, **20**, pp. 35–54

[26] Wu J., Uchida S., Fujishiro Y., Yin S., Sato T.: 'Synthesis and photocatalytic properties of $HTaWO_6$/(Pt,TiO_2) and $HTaWO_6$/(Pt,Fe_2O_3) nanocomposites', *Int. J. Inorg. Mater.*, 1999, **1**, pp. 253–258

[27] Wang L., Wu J., Huang M., Lin J.: 'Synthesis and photocatalytic properties of layered intercalated materials $HTaWO_6$/(Pt, $Cd_{0.8}Zn_{0.2}S$)', *Scr. Mater.*, 2004, **50**, pp. 465–469

[28] Mukherji A., Marschall R., Tanksale A., *ET AL.*: 'N-doped $CsTaWO_6$ as a new photocatalyst for hydrogen production from water splitting under solar irradiation', *Adv. Funct. Mater.*, 2011, **21**, pp. 126–132

[29] Chen X.B., Mao S.S.: 'Titanium dioxide nanomaterials: synthesis, properties, modifications, and applications', *Chem. Rev.*, 2007, **107**, pp. 2891–2959

[30] Li X., Kikugawa N., Ye J.: 'Nitrogen-doped lamellar niobic acid with visible light-responsive photocatalytic activity', *Adv. Mater.*, 2008, **20**, pp. 3816–3819

[31] Li X., Kikugawa N., Ye J.: 'A comparison study of rhodamine B photodegradation over nitrogen-doped lamellar niobic acid and titanic acid under visible-light irradiation', *Chem. Eur. J*, 2009, **15**, pp. 3538–3545

[32] Li G., Yang N., Wang W., Zhang W.F.: 'Synthesis, photophysical and photocatalytic properties of N-doped sodium niobate sensitized by carbon nitride', *J. Phys. Chem. C*, 2009, **113**, pp. 14829–14833

[33] Li Q., Yue B., Iwai H., Kako T., Ye J.: 'Carbon nitride polymers sensitized with N-doped tantalic acid for visible light-induced photocatalytic hydrogen evolution', *J. Phys. Chem. C*, 2010, **114**, pp. 4100–4105

[34] Govind V.K., Uma S.: 'Investigation of cation (Sn^{2+}) and anion (N^{3-}) substitution in favor of visible light photocatalytic activity in the layered perovskite $K_2La_2Ti_3O_{10}$', *J. Hazard. Mater.*, 2011, **189**, pp. 502–508

[35] Reddy J.R., Ravi G., Veldurthi N.K., *ET AL.*: 'Sol–gel synthesis and photocatalytic study of visible light active N-doped $KSbWO_6$', *Z. Anorg. Allg. Chem.*, 2013, **639**, pp. 794–798

[36] Ravi G., Veldurthi N.K., Palla S., Velchuri R., Pola S., Vithal M.: 'Synthesis, characterization and photocatalytic activity of $KAl_{0.33}W_{1.67}O_6$ and $Sn_{0.5}Al_{0.33}W_{1.67}O_6xH_2O$', *Photochem. Photobiol.*, 2013, **89**, pp. 824–831

[37] Ravi G., Veldurthi N.K., Muvva D.P., Munirathnam N.R., Prasad G., Vithal M.: 'Preparation, optical, and photocatalytic studies of defect pyrochlores: $KCr_{0.33}W_{1.67}O_6$ and $A_xCr_{0.33}W_{1.67}O_6$ nH_2O', *J. Nano. Part. Res.*, 2013, **15**, 1939 (doi 10.1007/s11051-013-1939-0)

[38] Qiu X., Burda C.: 'Chemically synthesized nitrogen-doped metal oxide nanoparticles', *Chem. Phys*., 2007, **339**, pp. 1–10

[39] Sun C., Mukherji A., Liu G., Wang L., Smith S.C.: 'Improved visible light absorption of $HTaWO_6$ induced by nitrogen doping: an experimental and theoretical study', *Chem. Phys. Lett*., 2011, **501**, pp. 427–430